npj | biomedical innovations

Article

https://doi.org/10.1038/s44385-025-00011-3

Super-lubricous polyethylene glycol hydrogel microspheres for use in knee osteoarthritis treatments

Samuel Stealey[1], Ether Dharmesh[1], Maitreyi Bhagat[2], Abdul Malik Tyagi[3], Andrew Schab[1], Melissa Hong[2], Damon Osbourn[2], Yousef Abu-Amer[3], Paul A. Jelliss[2] & Silviya Petrova Zustiak[1] ✉

Knee osteoarthritis (OA) is characterized by cartilage degeneration and significant reduction in lubrication. One strategy to recover the natural lubrication of the synovial fluid is the injection of hydrogel microspheres. Here, we have fabricated polyethylene glycol (PEG)-based hydrogel microspheres via a modified electrospraying setup. To improve throughout, crosslinking of PEG droplets was delayed until after droplet formation was complete. A custom-synthesized super-lubricious copolymer consisting of adhesive dopamine methacrylate (DMA), zwitterionic sulfobetaine methacrylate (SBMA), and fluorescent rhodamine B was used to dip-coat the PEG microspheres. Super-lubricious PEG microspheres coating reduced coefficient of friction by 57% compared to simulated synovial fluid, indicating beneficial lubrication properties. When injected into C57BL6 mice, PEG microspheres exhibited stability for up to 26 d and did not adversely affect mouse behavior. These super-lubricious PEG microspheres offer great promise to reduce the friction that is a hallmark of progressive OA, potentially mitigating the need for total knee arthroplasty.

Knee osteoarthritis (OA) is a debilitating disease that significantly alters the microenvironment of the knee, increasing inflammation and reducing lubrication[1,2]. This increased friction leads to significant wear and tear of articular cartilage, causing excruciating pain. Cartilage degeneration and inflammation proceed until a complete knee replacement is necessitated[2]. It is currently estimated that over 32 million people in the United States alone suffer from varying degrees of OA, totaling ~$185 billion in socioeconomic costs[3,4]. Furthermore, it is anticipated that 1 in 2 people will develop OA by the age of 85, resulting in over 72 million cases by 2030[3]. As such, innovative treatments are needed to slow the inflammation and articular cartilage degeneration that characterize OA and to potentially restore joint homeostasis.

Current strategies to alleviate osteoarthritis include injections of hyaluronic acid, platelet rich plasma, or other biologics that either seek to aid in the lubrication of the synovial joint or reduce inflammation[5–8]. However, these often suffer from a short residence time due to rapid clearance from the synovial cavity[9]. Even macromolecules such as proteins may be cleared within a matter of hours, while smaller molecules such as biologics can be cleared even faster. Progression of osteoarthritis can also further expedite the rate of clearance due to enhanced vascular permeability[10].

The injection of hydrogel microspheres within the synovial cavity has emerged as a tactic to treat OA[11]. Compressible microspheres can provide mechanical support to lessen the load exerted on cartilage during normal knee movement[12]. The water content and viscoelasticity can serve to absorb and dissipate mechanical forces, mimicking the natural cartilage. Growth factors may be incorporated within the hydrogels to modulate the microenvironment[13]. Hydrophilic hydrogel microspheres may also serve to restore some of the lubrication in the knee[14]. Lastly, hydrogel microspheres may be loaded with therapeutics to serve as a slowed release depot or with stem cells as a scaffold[15].

Here we developed super-lubricious polyethylene glycol (PEG) microspheres to alleviate the loss of lubricity within the synovial cavity. PEG offers tunable swelling, mechanical, and degradation properties, allowing for intentional design of microspheres[16–18]. Furthermore, biomolecules can be easily encapsulated and subsequently released in a sustained manner, while maintaining their bioactivity[19]. A Michael-type addition chemistry was used to crosslink PEG macromers and crosslinkers. Here, PEG microspheres were fabricated with a modified electrospraying setup, wherein gelation was delayed until after droplet formation and induced via addition of triethanolamine to the oil/PEG droplet mixture. These PEG microspheres were further coated with a custom-synthesized copolymer of

[1]Department of Biomedical Engineering, School of Science and Engineering, Saint Louis University, Saint Louis, MO, USA. [2]Department of Chemistry, School of Science and Engineering, Saint Louis University, Saint Louis, MO, USA. [3]Department of Orthopaedics, Washington University in Saint Louis, Saint Louis, MO, USA. ✉e-mail: silviya.zustiak@slu.edu

dopamine methacrylate and sulfobetaine methacrylate, namely poly(DMA-co-SBMA), offering a layer of polymer brush coating to improve the lubricity of the synovial fluid in the OA knee. We have evaluated the efficacy and stability of this coating, as well as the impact on microsphere mechanical properties.

Results

Poly(DMA-co-SBMA) was synthesized by a customized RAFT-mediated alkene polymerization initiated by AIBN with CAT acting as the RAFT agent, and isolated by dialysis against water (Fig. 1A). The methodology was adapted from a procedure reported by Wang et al. for the copolymerization of *N,N*-dimethylacrylamide with SBMA and, in this particular case, the addition of the RAFT agent greatly improved yield from <10% to >50% and eliminated the presence of small amounts of unreacted alkene reagents in the final product. Because all monomers were present at polymerization initiation, random incorporation through chain growth propagation was expected.

The resulting powder products isolated following dialysis were characterized using FTIR and ^{1}H NMR spectroscopies with the predominance of SBMA evident in both. The FTIR spectrum of poly(DMA-co-SBMA) can be compared to those of the SBMA and DMA monomers (Fig. 1B). Features attributable to SBMA (less those associated with the alkene C = C double bond) can clearly be identified, most notably the feature at 1038 cm^{-1} due to the SO_3 stretching mode. Most unique DMA absorptions (again less those associated with the alkene C = C double bond) are masked by SBMA resonances and so cannot be easily discerned in the FTIR spectrum of the polymers. The poly(SBMA-co-DMA) shows two broad swathes from 2800–3000 cm^{-1} due to C − H stretching and 3100–3600 cm^{-1} due to both O − H and N − H stretching modes. Because SBMA does not have active resonances in the region of 3200–3300 cm^{-1}, these absorptions can be attributed to the catechol O-H and amide N-H groups of DMA, pointing to the successful incorporation of DMA within the copolymer. Furthermore, the DMA amide C = O stretching resonance at 1525 cm^{-1} corresponds to a discernible resonance at this position in the polymer, again where there is a paucity of SBMA absorptions.

The ^{1}H NMR spectrum of a PBS/D_2O solution of poly(SBMA-co-DMA) revealed the strongest peaks that are aligned with those expected for the protons of polymer-incorporated SBMA and DMA (Fig. 1C). The benefit of including the RAFT agent in the polymerization protocol is realized by the absence of alkenic protons associated with unreacted monomers (Supplementary Fig. 1). Analysis of the peak integrals for the three DMA aromatic catechol ($C_6H_3(CH_2)(OH)_2$) protons (δ 6.7–7.2) compared with the six SBMA dimethylammonium ($((CH_2)_2N\mathit{Me}_2^+$) protons at δ 3.0 permitted determination of the SBMA:DMA monomer ratio of approximately 9:1 in the polymer, indicating that for polymer chains long enough to be entrapped by dialysis, the incorporation of DMA was less than that expected from the reaction ratios.

Size exclusion chromatography (SEC) was measured on a PBS solution of poly(DMA-co-SBMA) to gauge polymer molecular weight and polydispersity (Fig. 1D, E). Compared to a set of dextran-FITC standards (also

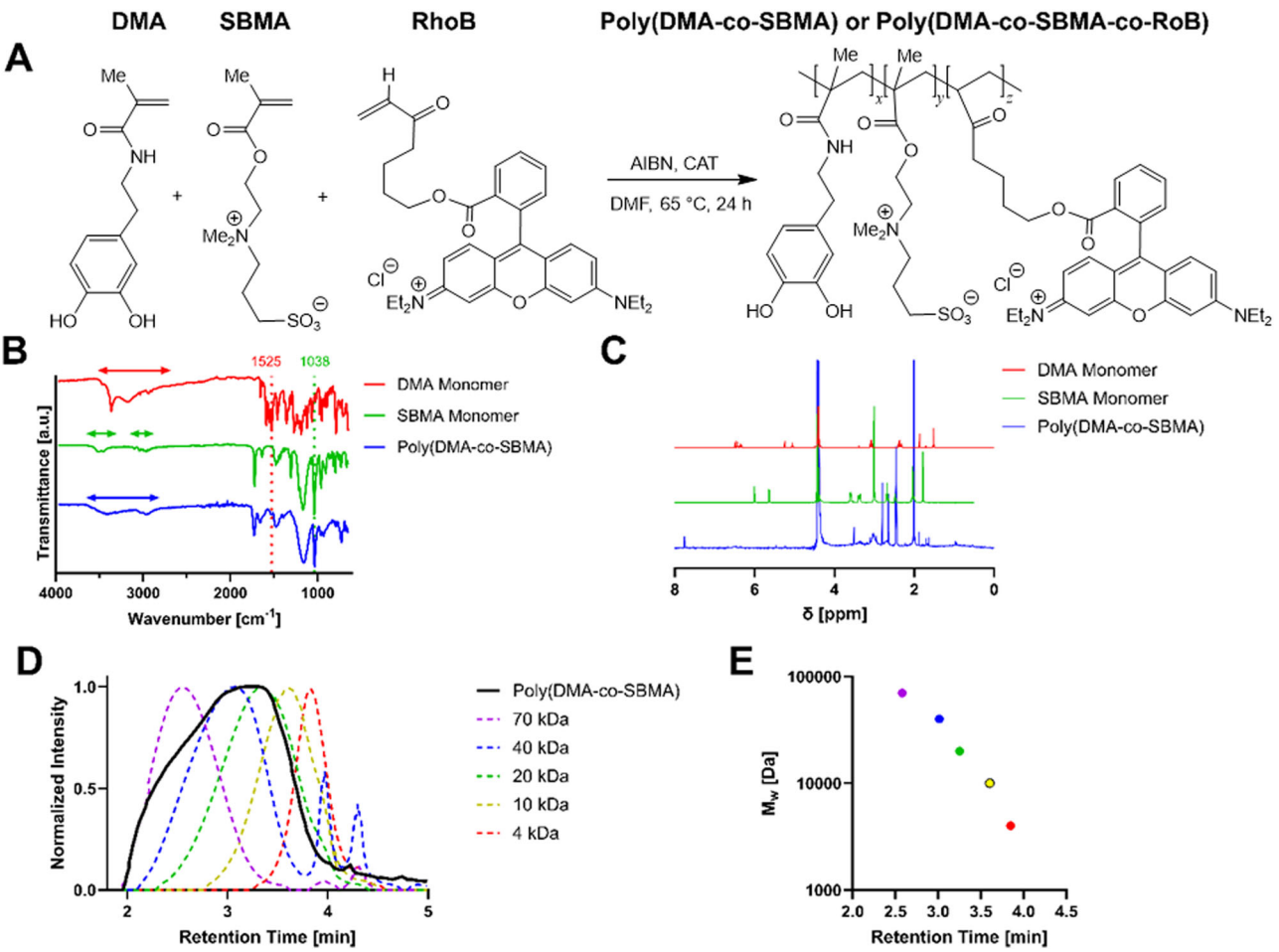

Fig. 1 | Synthesis and characterization of super-lubricious copolymer. A Synthesis of poly(DMA-co-SBMA) (*x*:*y* = 1:9, *z* = 0) and poly(DMA-co-SBMA-co-RhoB) (*x*:*y* = 1:9, *z* < 0.5%). **B** FTIR spectra of DMA monomer, SBMA monomer, and poly(DMA-co-SBMA). **C** ^{1}H NMR spectra of DMA monomer, SBMA monomer, and poly(DMA-co-SBMA). **D** SEC traces of poly(DMA-co-SBMA) and dextran standards and fitted standard curve (**E**).

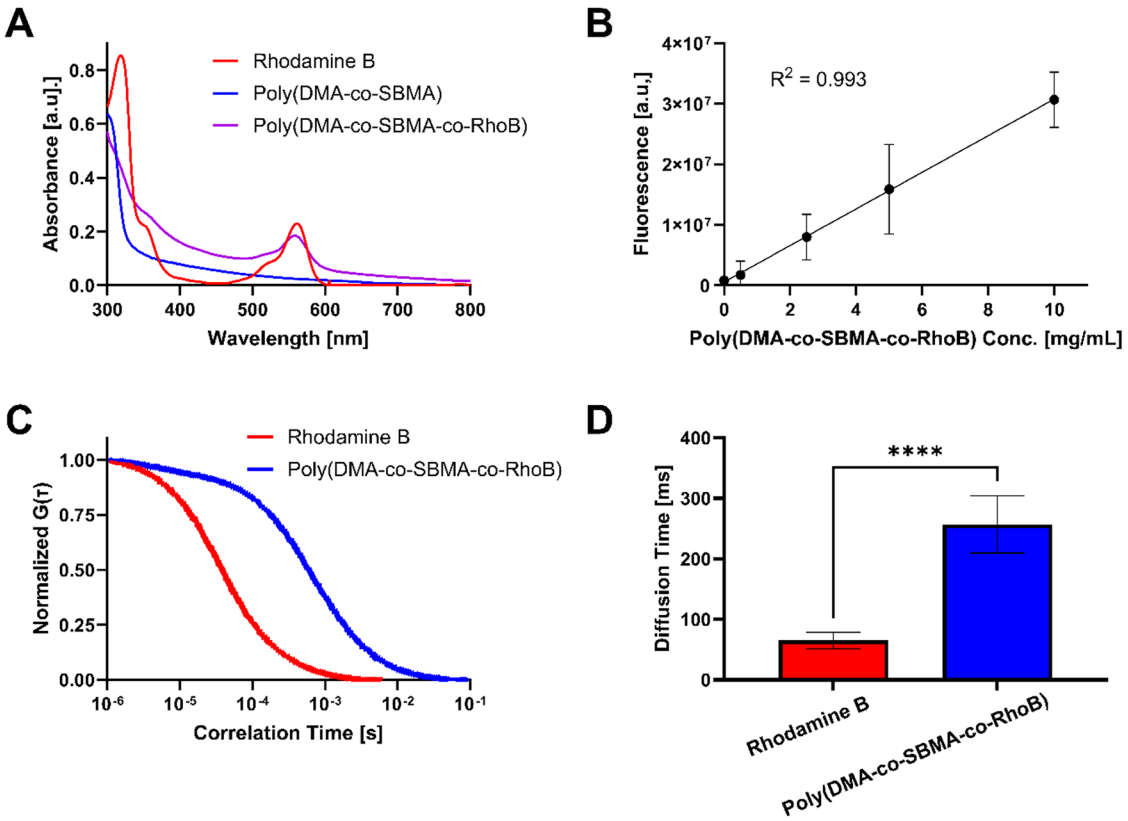

Fig. 2 | Characterization of super-lubricious copolymer with incorporated RhoB. **A** UV-vis spectra of RhoB, poly(DMA-co-SBMA), and poly(DMA-co-SBMA-co-RhoB). **B** Fluorescence intensity as a function of poly(DMA-co-SBMA-co-RhoB) concentration. **C** Normalized FCS autocorrelation curves for RhoB and poly(DMA-co-SBMA-co-RhoB). **D** Measured diffusion times of RhoB and poly(DMA-co-SBMA-co-RhoB). * indicates statistically significant difference, where $N = 4$ and $p < 0.05$.

run in PBS solution), the polymer molecular weight is somewhat polydisperse, with the bulk of the polymer chains (ca. 75%) having molecular weights ranging from 20 to 40 kDa and with ~25% in the 40–70 kDa range.

Although DMA contains a catechol chromophore in the dopamine segment of the molecule, to incorporate a fluorophore for the purpose of monitoring and tracking the polymer binding to PEG microspheres in vitro and in vivo, the polymerization was repeated using the same approach but inclusive of 0.44 mol% RhoB dye, synthesized by DCC coupling of RhoB with 4-hydroxybutylacrylate. A loading no greater than 0.5 mol% was chosen to provide sufficient fluorescence detection without modifying the overall structural properties of the resulting polymer. The resulting poly(-DMA-co-SBMA-co-RhoB) was also isolated by dialysis.

Because of the limited solubility of the polymer and the low mol % incorporation of RhoB, there were no spectroscopic resonances observed for the RhoB moiety in either the FTIR or the NMR spectra, which were essentially identical to those of the poly(DMA-co-SBMA) product (Supplementary Fig. 2). However, the solid product and its solutions retained a distinct light red hue attributable to the RhoB fluorophore (Supplementary Fig. 3). The presence of RhoB residues was nevertheless confirmed by UV-vis spectroscopy on PBS solutions of the polymer which shows near identical visible region absorptions to that of the RhoB acrylate monomer (λ_{max} = 561 nm with a shoulder at ca. 520 nm), while the poly(DMA-co-SBMA) with no incorporated dye showed no absorptions at all in this region (Fig. 2A).

Copolymer fluorescence was also shown to correlate linearly with poly(DMA-co-SBMA-co-RhoB) concentration (Fig. 2B). FCS was also used to confirm successful incorporation of RhoB into the poly(DMA-co-SBMA-co-RhoB) chain. Our data showed that diffusion was significantly slowed for poly(DMA-co-SBMA-co-RhoB) compared to free RhoB, as evidenced by a 4-fold increase in diffusion time (Fig. 2C, D). Slower diffusion was expected for the large polymer chain compared to the small molecule free dye. The results confirm that the copolymer solution was fluorescent due to the dye being chemically incorporated into the polymer structure as opposed to residual unreacted RhoB being present in the copolymer solution.

A modified electrospraying setup was used to fabricate PEG hydrogel microspheres, which were subsequently dip-coated with the super-lubricious copolymer (Fig. 3A, Supplementary Fig. 4). To prepare the PEG microspheres, 4-arm PEG-Ac and PEG-diSH were reacted via Michael type addition to form a chemically crosslinked microsphere network. Under physiologic conditions at pH 7.4, gelation typically proceeds in about 15 min for a 10% w/v polymer solution as the one used here. However, this was an impediment for electrospraying, where 4-arm PEG-Ac and PEG-diSH were pre-mixed and added to the same syringe. When doing so, polymer chain lengthening and crosslinking proceeded within the syringe, limiting the run time to ~10 min before increased solution viscosity negatively affected droplet polydispersity and syringe needles became occluded. To alleviate this issue, 4-arm PEG-Ac and PEG-diSH were pre-mixed at pH 5.5, greatly slowing the Michael-type addition process to a gelation time of >2 h (Supplementary Fig. 5). As such, electrospraying could proceed uninterrupted, leading to longer run times and reduced droplet polydispersity. PEG droplets were collected in an oil collection bath under constant stirring to minimize PEG droplet coalescence and aggregation. The oil collection bath contained TEA, which diffused into the PEG droplets from the surrounding oil phase, effectively raising the pH of the aqueous droplet phase. This allowed the gelation of PEG droplets in <10 min, forming stable PEG microspheres. Without the addition of TEA to the oil phase, PEG droplets did not undergo gelation and were not stable following buffer exchange into aqueous PBS. Once microspheres were gelled, no further coalescence of microspheres was observed.

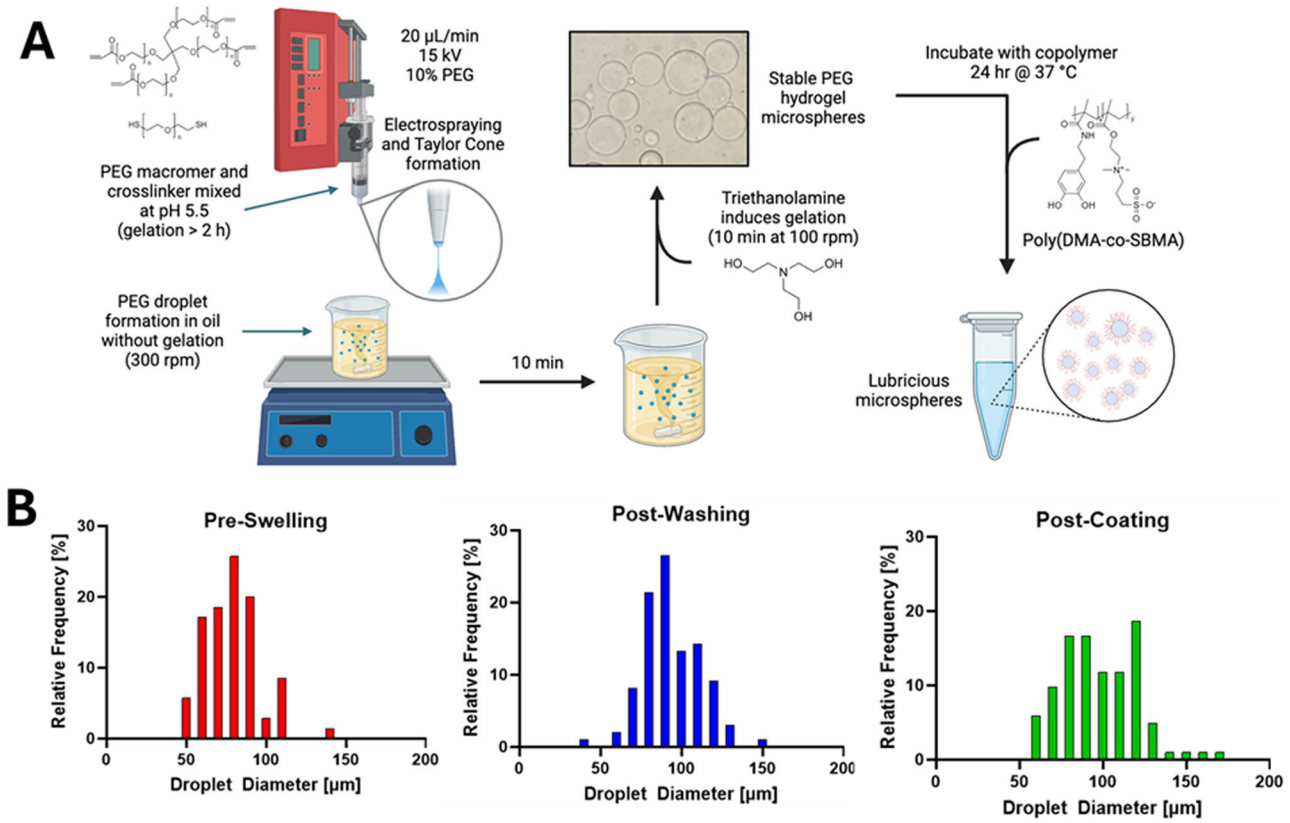

Fig. 3 | Fabrication of super-lubricious copolymer-coated PEG hydrogel microspheres. A Schematic of the electrospraying process, in which PEG macromer (4-arm PEG-Ac) and crosslinker (PEG-diSH) were mixed in reduced pH buffer to prevent gelation within the syringe. Following droplet formation, TEA was added to the collection bath, inducing gelation within 10 min. PEG microspheres were subsequently dip-coated with poly(DMA-co-SBMA) copolymer. **B** Histogram of PEG droplet/microsphere size prior to washing, after washing, and following copolymer coating.

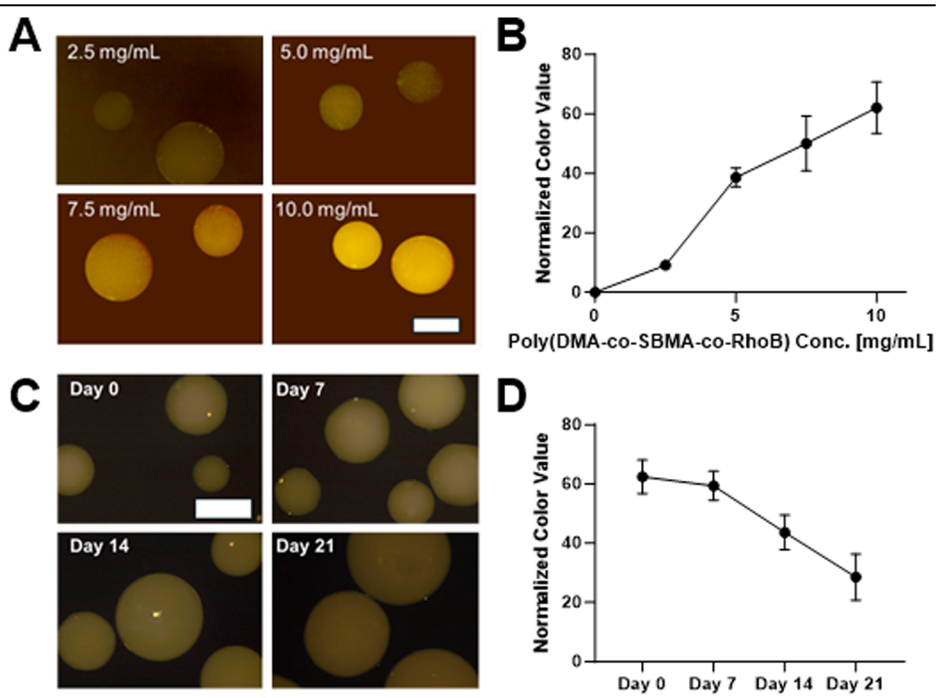

Fig. 4 | Poly(DMA-co-SBMA-co-RhoB) coating of PEG microspheres. A Widefield fluorescent microscopy imaging of PEG microspheres dip-coated with varying concentrations of poly(DMA-co-SBMA-co-RhoB). Scale bar represents 100 µm. **B** Quantification of fluorescence from fluorescence imaging as a function of copolymer concentration. **C** Widefield fluorescent microscopy imaging of PEG microspheres dip-coated with 10 mg/mL poly(-DMA-co-SBMA-co-RhoB) over time. Scale bar represents 100 µm. **D** Quantification of fluorescence from fluorescence imaging of microspheres over time.

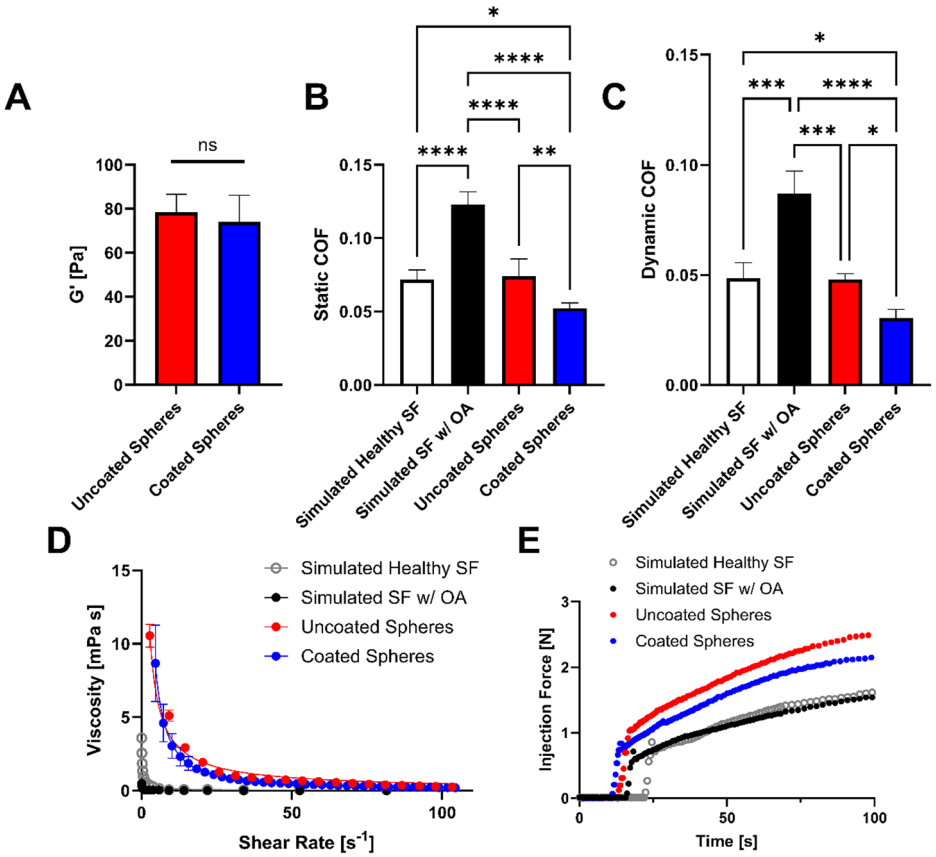

Fig. 5 | Mechanical characterization of PEG microspheres. A Stiffness of uncoated PEG microspheres and microspheres coated with poly(DMA-co-SBMA). **B** Measured static coefficient of friction and **C** dynamic coefficient of friction of uncoated microspheres and microspheres coated with poly(-DMA-co-SBMA) compared to simulated healthy and simulated osteoarthritic synovial fluid. * indicates statistically significant difference between indicated groups ($N = 4$, $p < 0.05$). **D** Viscosity of microsphere slurry solutions versus simulated synovial fluid as a function of rheological shear rate. **E** Force required for extrusion through a 27 G needle tip of uncoated and coated PEG microspheres compared to simulated synovial fluid.

PEG droplets exhibited relatively low polydispersity, with a diameter of 79 ± 17 µm and a coefficient of variance of ~18% (Fig. 3B). Hydrogel microspheres increased in size by 25% to 94 ± 18 µm due to swelling following washing. No significant difference in microsphere diameter, polydispersity, or swelling ratio was noted compared to microspheres made with PEG mixed with TEA prior to electrospraying (data not shown). Copolymer coating did not have a significant effect on microsphere size, with an average microsphere diameter for coated microspheres of 98 ± 22 µm. Several electrospraying parameters could be modified to vary the resulting PEG droplet and microsphere size, including voltage, flow rate, operating height, and syringe needle diameter. Here, we investigated the lattermost of these options and showed that decreasing the needle diameter decreased PEG droplet size while improving polydispersity (Supplementary Fig. 6). This reduction in variation of droplet size could be attributed to dripping occurring during the electrospraying process for larger needles.

To further confirm copolymer adsorption onto PEG hydrogel microspheres, fluorescent imaging was performed on poly(DMA-co-SBMA-co-RhoB)-coated microspheres (Fig. 4A, B). Fluorescence from the copolymer was clearly co-localized with the microspheres, with virtually all microspheres exhibiting some fluorescence. As expected, as poly(DMA-co-SBMA-co-RhoB) dip-coating concentration increased, so did fluorescence of the coated microspheres, indicative of successful copolymer adsorption on the PEG microspheres. Small pockets of relatively bright fluorescence observed on the surface of some microspheres was attributed to incomplete dissolution of poly(DMA-co-SBMA-co-RhoB). Confocal imaging revealed that poly(DMA-co-SBMA-co-RhoB) was not only adsorbed to the surface of microspheres, but was also seen in the interior of the PEG microspheres (Supplementary Fig. 7). However, fluorescence was higher near the edges of the microspheres, indicating that the copolymer was incorporated by predominantly surface adsorption.

Microspheres showed good dispersibility, with only gentle perturbation via pipetting resulting in individual microspheres and little to no aggregation, as shown with microscopy images. Zeta potential analysis (Supplementary Fig. 8) further revealed a decrease in zeta potential following poly(DMA-co-SBMA) adsorption, indicating a trend toward enhancement in repulsion between microspheres, as well as further demonstrating successful adsorption of the copolymer.

Copolymer coating of microspheres was also shown to be stable for at least 21 days (Fig. 4C, D). No significant change in microsphere fluorescence (or size) was observed over the first 7 days. By Day 14 and Day 21, a decrease in fluorescence was measured, accompanied by an increase in microsphere diameter. The increase in size could be attributed to hydrolytic degradation of the PEG mesh structure, leading to increased swelling. The degradation of PEG microspheres may also be responsible for the release of adsorbed copolymer and decrease in fluorescence signal. Furthermore, the increase in size of microspheres reduced the effective copolymer concentration, as the same mass of copolymer was spread onto a larger surface area.

Rheological and tribological measurements of coated and un-coated PEG microspheres were performed to evaluate the mechanical properties of microsphere slurry solutions. For rheological measurements, validation was performed to ensure the geometry gap used was compressing microspheres, rather than just the solution above the microspheres (Supplementary Fig. 9). Copolymer coating of PEG microspheres did not significantly affect microsphere stiffness (Fig. 5A, Supplementary Fig. 10). Tribological measurements were performed with a custom tribo-rheology setup to quantify the coefficient of friction in comparison to simulated healthy and simulated osteoarthritic synovial fluid. These fluids represented the typical loss in HA and reduction in viscosity associated with OA. As was expected, healthy SF exhibited lower COF compared to simulated osteoarthritic SF, demonstrating the significant loss in lubricity that exemplifies OA progression. (Fig. 5B, C). Uncoated PEG microspheres exhibited similar COF to healthy SF, while poly(DMA-co-SBMA) coating of microspheres significantly improved lubricity compared to uncoated spheres (20% reduction in dynamic coefficient of friction). Furthermore, coated microspheres reduced

dynamic coefficient of friction 26% compared to simulated healthy SF and 65% compared to simulated osteoarthritic SF. Both uncoated and coated PEG microspheres also exhibited shear-thinning behavior as indicated by a reduction in viscosity with increasing shear rate (Fig. 5D). This shear-thinning behavior was also evident by the relatively low injection force needed to extrude the microsphere slurries through a 27 G syringe needle (Fig. 5E). While both uncoated and coated microspheres required more force for injection compared to simulated osteoarthritic and simulated healthy synovial fluid, excessive force was not required for microsphere injection and no occlusions of the needle were noted. Coated microspheres required slightly less injection force than the uncoated microspheres, potentially due to the increased lubricity imparted by the copolymer coating.

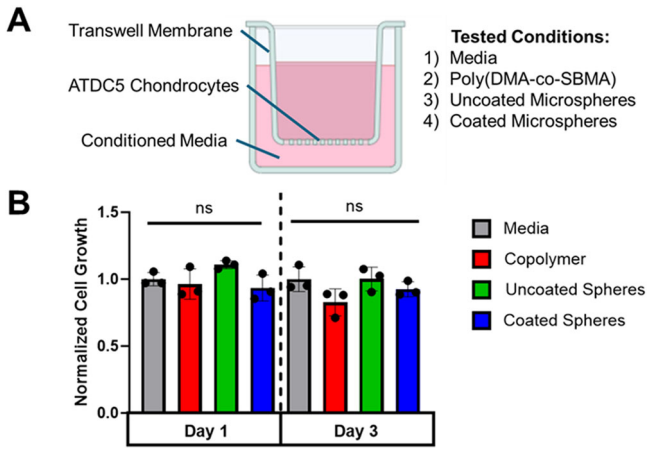

Fig. 6 | In vitro cytotoxicity of coated and uncoated PEG microspheres. **A** Schematic of assay setup, in which cells were cultured on transwell plates with conditioned media in each well. **B** MTS assay quantification of cell viability in each condition after 1 d and 3 d of exposure ($p < 0.5$, $N = 4$).

In vitro cytotoxicity of microspheres and copolymer coating was evaluated using an MTS growth assay with ATDC5 chrondrocytic cells (Fig. 6). Cells were cultured on a transwell plate and exposed to media only, media + 10 mg/mL poly(DMA-co-SBMA), media + uncoated PEG microspheres, or media + PEG microspheres coated with 10 mg/mL poly(DMA-co-SBMA). No significant differences in cell viability were observed between the media only and copolymer or microsphere-containing samples, indicating these components did not significantly alter cell growth.

Super-lubricious PEG hydrogel microspheres were injected in the knees of mice to evaluate their in vivo stability and biocompatibility. To allow for fluorescent imaging in the near infrared region, PEG microspheres were loaded with near-infrared fluorescent spheres (~100 nm). To compare to a sham injection, contralateral legs were injected with PBS with a comparable concentration of fluorescent spheres (Fig. 7A, B). A strong fluorescent signal was preserved over the period of 26 days for the hydrogel microsphere group, indicating a long resident time within the synovial cavity. The PBS (no microsphere) group showed longer persistence of fluorescence than was expected. This could be attributed to longer residence times of the fluorescent spheres (diameter = 100 nm) compared to biomolecules (diameter < 10 nm). Contralateral legs exhibited 1000-fold reductions in fluorescence compared to initial fluorescence values of injected legs, though these fluorescent values did not change over time.

A static weight bearing test was also performed on these mice to determine if the injection of the hydrogel microspheres negatively affected mouse quality of life (Fig. 7C). No significant difference was observed between the PBS only and the microsphere groups, indicating the microspheres were not adversely affecting mouse behavior.

Discussion

The development of super-lubricious microspheres allows for an easily injectable method to alleviate friction that accompanies progressive osteoarthritis. Here, we have developed tunable PEG microspheres with a lubricious copolymer coating, further enhancing the lubricious nature of the microspheres.

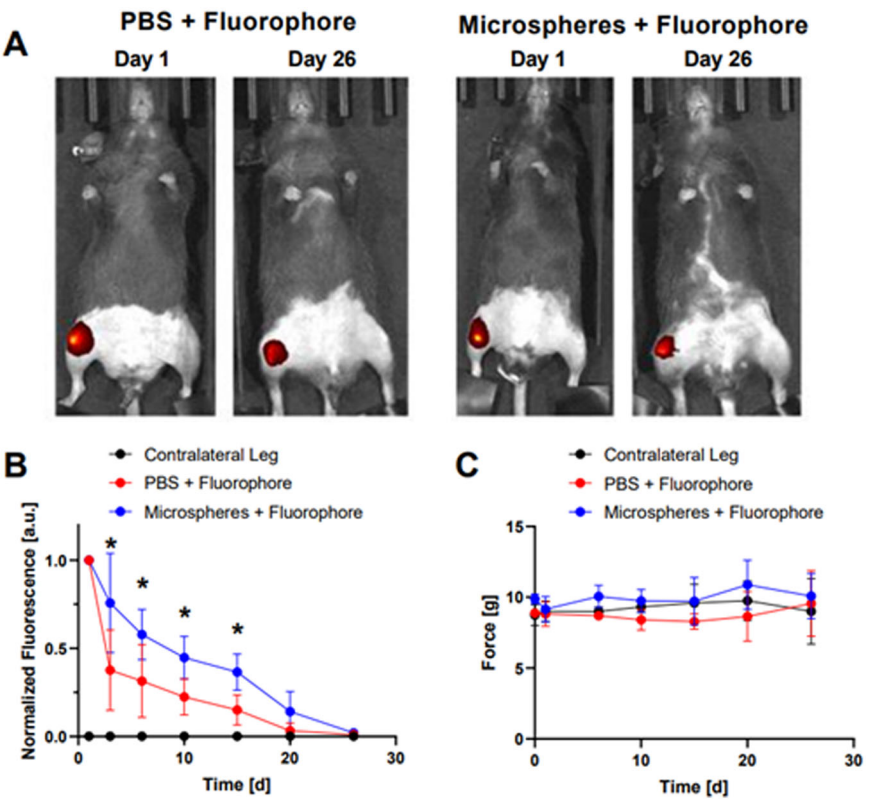

Fig. 7 | In vivo testing of poly(DMA-co-SBMA)-coated PEG microspheres. **A** IVIS imaging of fluorescent microspheres compared to free fluorescent particles on Days 1 and 26. **B** Quantification of IVIS fluorescence over time. Total radiant efficiency was normalized to the value on Day 1 for each respective mouse. Contralateral legs were normalized to the fluorophore containing-leg's initial fluorescence. **C** Pain assessed by static weight bearing test for mice injected with PBS or PEG microspheres. * indicates statistically significant difference between PBS and Microsphere groups ($N = 5$, $p < 0.05$).

A modified delayed electrospraying setup was used to fabricate these PEG microspheres via Michael-type addition. This reaction, in which a nucleophile attacks an electrophilic alkene or alkyne, is quite beneficial to developing PEG hydrogels with varying gelation, degradation, and mechanical properties, as PEG end-groups can easily be substituted as needed[17,20]. By delaying gelation of PEG until after droplet formation, extrusion can continue well beyond the typical time at a PEG precursor solution of pH 7.4. Thus, the method offers a one-syringe, high throughput method. This allows for a simpler setup compared to some microfluidic chip devices that have been developed in which PEG macromer and crosslinker are injected in separate syringes[21,22].

Microspheres provide a number of benefits that lend themselves to use for the treatment of OA. A variety of polymers, both natural and synthetic, have been used to fabricate compressible microspheres[23,24]. This property allows the microspheres to absorb the relatively large loads that accompany normal knee functionality and support cartilage. The small size of microspheres also allows for filling of irregular spaces on the surface of and in defects on articular cartilage that may not be possible for bulk hydrogels[25,26]. Microspheres can also be injectable, allowing for simpler, safer, and less intrusive administration compared to bulk hydrogel implantation[27].

Perhaps the most important functionality of microspheres for treatment of OA is their lubrication properties. Age-related factors or traumatic injuries in the knee can lead to increased shear strain on cartilaginous cells and an upregulation of cartilage-degrading enzymes[28]. As articular cartilage degrades, higher sliding friction further upregulates catabolic enzymes, resulting in a self-propagating cycle in which cartilage is further damaged[29].

These hydrogel microspheres would likely not completely replace the full volume of the synovial cavity, but rather form a dynamic coating layer across the cartilaginous joint surface. As OA progresses, the joint space can exhibit irregular cavities that could be filled by the hydrogel microspheres[30]. Furthermore, it is unlikely that the injected hydrogel microspheres remain in place during the repetitive mechanical perturbation of normal knee movement. Rather, the hydrogel microspheres may exhibit mobility in response to applied stresses. Careful consideration of microsphere concentrations represents an important parameter that must be optimized to maximize therapeutic effectiveness.

While the polymeric microspheres themselves can aid in reducing friction in the synovial cavity, coating the microspheres can further improve lubricity[14,31]. In addition to reducing friction compared to bare microspheres, this coating layer must be able to stick effectively to the microspheres to maintain its therapeutic effect. If the coating is only loosely bound to the microspheres, the beneficial lubricity may be cleared from the synovial cavity. Lubricious coatings may also serve to prevent coalescence and aggregation of microspheres, further improving their injectability. Such results were observed here, with virtually no microsphere aggregation shown by microscopy and a decrease in zeta potential following poly(DMA-co-SBMA) coating.

We have also successfully incorporated a fluorophore within the polymeric structure, allowing for easy visual and spectroscopic identification of the copolymer. Without the incorporated Rhodamine B more involved techniques such as ^{1}H NMR would be required to evaluate the efficacy and stability of the copolymer coating. While Rhodamine B was used here, other fluorophores could also potentially be incorporated to accommodate other imaging modalities or in conjunction with other fluorescent stains[32,33]. Importantly, the copolymer structure was not adversely affected by the incorporation of the fluorophore.

The poly(DMA-co-SBMA-co-RhoB) coating was shown to be stable in vitro for at least 21 days. While fluorescent microscopic analysis revealed some copolymer did desorb and was released from the PEG microspheres, this released copolymer would not be expected to adversely affect the local environment nor cause cytotoxicity[34], which was confirmed by our in-vitro cell viability assay. Contrarily, because poly(DMA-co-SBMA) itself is lubricious, even released copolymer could contribute to reduced friction in the synovial cavity.

PEG microspheres showed stability in vivo for up to 26 days in a murine model, without causing any adverse effects on mouse behavior or health. Such a residence time could allow for relatively infrequent monthly injections. These PEG microspheres degrade via hydrolytic degradation of the thioester bond formed between 4-arm PEG-Ac and PEG-diSH. In vitro, this degradation typically takes ~25 days at 37 °C[22]. However, the complex microenvironment of the synovial cavity and the presence of intense mechanical perturbations could alter this degradation time. Changing the PEG formulation could also extend the degradation time of the microspheres, presumably without negative effect on microsphere lubricity[16]. For comparison, current hyaluronic acid treatments are used on variable treatment schedules, from weekly injections to doses every six months[35]. The degradation time of polymeric microspheres for OA treatment has a similarly high variability. Thus, the degradation profile and residence time of these coated PEG microspheres is suitable for OA treatment.

It is unlikely that these PEG microspheres would be rapidly cleared from the synovial cavity via lymphatic drainage due to their relatively large size compared to individual polymers[36]. However, PEG polymers <40 kDa can be cleared via renal excretion or the lymphatic system due to their relatively small size[36]. The degradation products of the PEG polymers used here could be expected to be cleared in this manner as their molecular weights of <10 kDa fall well beneath this threshold. The retention time of our PEG microspheres in the synovial cavity is comparable to that of hyaluronic acid-based hydrogel microspheres of similar size utilized by Lei et al. [27] and, separately, Xiao et al.[30].

Such a residence time can also allow for diffusion-controlled release of encapsulated therapeutics if the microspheres were to be used as drug delivery devices[8,37]. For example, Choi et al. demonstrated encapsulated platelet-rich plasma (PRP) was released within 20 d from similar PEG hydrogels[38]. It is desirable for microsphere carriers to outlast the complete release time of the encapsulated cargo to ensure predictable release kinetics as microspheres degrade. Here, the degradation time of the PEG microspheres is only slightly longer than the release times, allowing for repetitive injections to maintain lubrication in the synovial cavity as well as continuous release of biomolecules that may be incorporated into the microspheres in future iterations.

Mechanical testing of PEG microspheres with and without poly(DMA-co-SBMA) copolymer coating showed enhanced lubricity compared to a simulated osteoarthritic synovial fluid. This is indicative of the PEG microspheres themselves reducing friction (39% reduction in SCOF compared to SF), while the copolymer further enhanced the lubricity (29% reduction in SCOF compared to uncoated microspheres). These results are similar to those obtained with a DMA/SBMA coating applied to gelatin methacrylate spheres[34]. The enhanced lubricating properties of the copolymer coating can be attributed to the zwitterionic nature of the SBMA monomers, which form a strong hydration brush layer[39,40].

It is important for microspheres to be used for treatment of osteoarthritis to maintain their stability and lubricity even under the high pressures during loading in the synovial cavity. The compression of microspheres could lead to changes in aggregation and "filter-pressing", in which water is expelled and microspheres become stiffer. Here, friction was measured at relatively high contact pressures (~1 GPa), which is significantly higher than the physiological contact pressure of approximately 1–10 MPa[41]. As such, any change in microsphere size, aggregation, or water retention would be accounted for during these coefficient of friction measurements.

These poly(DMA-co-SBMA)-coated PEG microspheres offer great promise for use in the alleviation of increased friction that is typical of knee osteoarthritis. The custom-synthesized copolymer coating provided a stable lubrication layer that significantly reduced the measured coefficient of friction while not eliciting adverse effects in a mouse model. This improvement of lubrication may slow the progression of OA, lessening the need for total knee arthroplasties. Future work will focus on optimizing the copolymer structure to maximize adsorption efficiency and lubrication properties. This PEG microsphere platform also lends itself to the encapsulation of therapeutics, significantly extending their residence time with the

synovial cavity. For example, PRP has been successfully encapsulated within similar microspheres by our group and demonstrated prolonged release. Upcoming studies will also investigate the distribution of microspheres within the synovial cavity in an OA mouse model, as well as the stability of these microspheres following the cyclic loading accompanied by knee motion. Lastly, the pathology and mouse response to these microspheres will be evaluated in comparison to non-treated animals.

In summary, we have successfully developed super-lubricious copolymer-coated PEG hydrogel microspheres. The custom-synthesized copolymer incorporated fluorescent RhoB, allowing for easy characterization of copolymer coating efficacy and stability. A modified delayed gelation electrospraying setup was implemented to allow for high throughput microsphere fabrication. Cell proliferation was shown to be unaffected by the presence of microspheres or copolymer coating. In vitro mechanical testing revealed coated hydrogel microspheres exhibited shear-thinning properties and reduced coefficient of friction by nearly 60% compared to simulated synovial fluid. Coated microspheres remained stable within the synovial cavity for up to 26 d in a mouse model and did not elicit adverse effects on mouse behavior. Our results indicate that the developed microspheres offer a great potential for use in knee osteoarthritis treatments.

Methods

Materials

Polyethylene glycol tetraacrylate (4-arm PEG-Ac; 10 kDa) and polyethylene dithiol (PEG-diSH; 3.4 kDa) were purchased from Laysan Bio (Arab, AL, USA). Vegetable oil was obtained from a local grocer. Triethanolamine (TEA) and fluorescent particles (Fluoro-Max Dyed Blue Aqueous Fluorescent Particles, 0.1 μm) were acquired from Sigma-Aldrich (Saint Louis, MO, USA). CoverWell perfusion chamber gaskets were purchased from Grace Bio-Labs (Bend, OR). Sulfobetaine methacrylate (SBMA, 3-[[2-methacolyloxy)ethyl]dimethylammonio]propane-1-sulfinate, >98.0%), dopamine methacrylamide (DMA, N-(3,4-dihydroxyphenethyl)methacrylamide, >98.0%), and 4-hydroxybutylacrylate (HBA, >97.0%),were purchased from TCI Chemicals (Portland, OR, USA). 2,2'-azodiisobutyronitrile (AIBN) was purchased from Chem Service Inc. (West Chester, PA, USA). 2-Cyano-2-propyl dodecyl trithiocarbonate (CAT, 97%), 1,3-dicyclohexylcarbodiimide (DCC, 99%), 4-dimethylaminopyridine (DMAP), Rhodamine B (RhoB, ≥95%), sodium bicarbonate ($NaHCO_3$, ACS reagent), sodium sulfate, anhydrous (Na_2SO_4, ACS reagent) and silica gel (70-230 mesh, 60 Å) were purchased from Millipore Sigma (St. Louis, MO, USA). Solvents: dimethylfomamide (DMF, >99.8%, Millipore Sigma (St. Louis, MO, USA)) was distilled under argon over 4 A molecular sieves (Millipore Sigma (St. Louis, MO, USA)), isopropyl alcohol (iPrOH, ACS reagent, Fisher Chemical) was used as supplied, methylene chloride (CH_2Cl_2, ACS reagent, Fisher Chemical) was distilled under argon over anhydrous $CaCl_2$ (Millipore Sigma (St. Louis, MO, USA)). Deuterium oxide (D_2O, 99.9%D) was purchased from Millipore Sigma (St. Louis, MO, USA). Deuterated phosphate buffer saline (PBS/D_2O) was made by dissolving sufficiently high purity PBS in D_2O to make a pD 7.8 solution. Dulbecco's Modified Eagle's Medium with F12 (DMEM/F12), fetal bovine serum (FBS), and snakeskin dialysis tubing (3.5k MWCO, 35 mm dry diameter) were purchased from Thermo Fisher Scientific (Rockford, IL, USA). ATDC5 chondrocytic cells derived from mouse embryonal carcinoma were obtained from Riken Cell Bank (Tsukuba, Japan). Penicillin streptomycin (pen-strep) was purchased from Hyclone, (Pittsburgh, PA, USA). 3-(4,5-dimethylthiazol-2-yl)-5-(3-carboxymethoxyphenyl)-2-(4-sulfophenyl)-2H-tetrazolium (MTS) assay was procured from Promega (Madison, WI, USA). 24-well transwell plate inserts (1.12 cm^2 growth area and 3 μm pore size) were purchased from Millipore Sigma (Saint Louis, MO, USA).

Synthesis of Poly(DMA-co-SBMA). The following synthesis is based on a modification of a method reported by Wang et al. and carried out using Schlenk-line procedures under an inert atmosphere of argon[42]. A 100 mL 3-necked round-bottom flask was fitted with a condenser and charged with 0.200 g (0.904 mmol) DMA, 0.800 g (2.87 mmol) SBMA, 10 μL CAT, and 40 mL of DMF. These quantities provide an SBMA-DMA molar ratio of 3:1. This mixture was heated to 65 °C using a digital temperature controller while stirring for 15–30 min. After this time, 5.0 mg (0.030 mmol) AIBN was added along with an additional 10 mL of DMF and then stirred at 65 °C for 24 h. The resulting solution was cooled to room temperature and then dialyzed against water at 25 °C for 5 days, with the water changed at 12 and 24 h and then once a day after that. The contents of the dialysis bag were then lyophilized to yield ~500 mg of white powder (or ~50% yield).

Synthesis of Rhodamine B Butylacrylate. The following synthesis is based on a modification of a method reported by Ward et al.[43] To a 100 mL round bottom flask, equipped with a magnetic stirring bar, was added 3.00 g (6.26 mmol) of RhoB and 40 mL of anhydrous CH_2Cl_2 solvent. The mixture was stirred, under argon, until the RhoB dye was dissolved. DMAP (0.080 g, 0.65 mmol) was then added to the flask, along with 1.50 mL (1.6 mol eq) of HBA. The mixture was then cooled to 0 °C, and 6.26 mL of DCC (1.0 M solution in CH_2Cl_2, 1 mol eq) was injected into the reaction flask with stirring. The reaction was held at 0 °C for 30 min, then allowed to slowly warm to room temperature, and finally stirred under nitrogen overnight. It was noted that the reaction by-product dicyclohexylurea (DCU) began to precipitate from solution shortly (~3 min) after the addition of the DCC. At the end of the reaction period the solution was filtered through a Celite plug. The CH_2Cl_2 solution was then extracted with 1.0 M sodium bicarbonate solution. After separation, the aqueous fraction was washed 2 times with CH_2Cl_2. The combined CH_2Cl_2 extracts were then washed with the 0.1 M $NHCO_3$ solution and then once with DI water and to this was added sufficient Na_2SO_4 to absorb residual traces of water. The wet Na_2SO_4 was removed by filtration and then the CH_2Cl_2 solvent was reduced in volume to ~15 mL on a rotary evaporator. This solution was then chromatographed on a silica gel (60–230 mesh) column. Elution afforded a preliminary weak red fraction which was discarded, followed by the main red fraction containing the product. A tertiary fraction following that, contained some unreacted RhoB and was not collected. After removal of the main product fraction, the solvent was removed with a rotary evaporator to leave a sticky red solid, which was dried *in vacuo*. Product identification was confirmed by ^1H and ^{13}C NMR spectroscopy. A 5.17 mM stock solution of the product was prepared in distilled DMF and used in subsequent polymerization procedures. Peak assignments are shown in the caption of Supplemental Fig. S3.

Synthesis of poly(DMA-co-SBMA-co-RhoB). Using the same reagent and solvent quantities and following the same procedure as for the synthesis of poly(DMA-co-SBMA) above, but with addition of 3.20 mL of a 5.17 mM RhoB butylacrylate solution to the initial reaction mixture, lyophilization of the final dialyzed mixture afforded ~700 mg of light red powder (or ~70% yield).

Characterization of Super-Lubricious Copolymer

Fourier Transform Infrared (FTIR) spectroscopy was performed using a Shimadzu FTIR-8400S spectrometer on compressed KBr pellets containing 5 mg polymer per 200 mg KBr. Nuclear magnetic resonance (NMR) spectroscopy was performed using a Bruker Avance 400 MHz NMR spectrometer on solutions of the polymers in 0.01 *M* PBS in D_2O (pD 7.8). UV-vis spectroscopy was carried out with a Shimadzu UV-2501PC spectrophotometer on 1 mg/mL solutions of the polymers in 1:1 DMF/H_2O. SEC was performed with an Agilent Bio SEC-3 HPLC column (100 Å pore size, 3 μm particle size, 7.8 × 50 mm (diameter × length)). A calibration plot was generated by separately chromatographing a set of 5 dextran standards labeled with fluorescein isothiocyanate (dextran-FITC) with listed molecular weights of 4, 10, 20, 40, and 70 kDa ± 1 kDa (TDB Labs, Sweden). All mobile phases were 0.1 *M* pH 7.4 PBS. A 1 mg/mL PBS solution of poly (DMA-co-SBMA-co-RhoB) was then chromatographed. Retention times were measured by monitoring eluant absorption at λ_{max} = 224 nm. UV-vis

spectroscopy was also used to confirm RhoB incorporation within poly-(DMA-co-SBMA) to form poly(DMA-co-SBMA-co-RhoB). Absorbance was measured at wavelengths of 300–800 nm using a SpectaMax i3 (Molecular Devices, San Jose, CA).

Fluorescence correlation spectroscopy (FCS) was also used to confirm incorporation of RhoB into the poly(DMA-co-SBMA) structure. To do so, samples of RhoB and poly(DMA-co-SBMA-co-RhoB) were diluted in PBS to 0.2 nM and 32 nM, respectively. Samples (40 µL) were pipetted into perfusion chamber gaskets capped to avoid evaporation. FCS measurements were performed with a Microtime200 (PicoQuant, Berlin, Germany) confocal microscope. Confocal volume (1.12–1.43 fL) was calibrated using free RhoB. A 547 nm pulsed laser was used at an optical power of ~10 µW for at least eight measurements of 120 s for each sample. An autocorrelation function $G(\tau)$ was obtained for each measurement[44]:

$$G(\tau) = \frac{1}{N}\frac{1}{\left[1+\left(\frac{\tau}{\tau_D}\right)\right]}\frac{1}{\left[1+p\left(\frac{\tau}{\tau_D}\right)\right]^{0.5}} \quad (1)$$

where N is the number of fluorescent particles, $p = r_o/z_o$ is an instrumental constant, r_o is the radius and z_o is the axial length of the focused laser beam spot, and τ_d is the solute diffusion time. The autocorrelation function was normalized for each measurement as $G(\tau_D) / G(\tau_0)$, where $G(\tau_D)$ is the value of Eq. 1 at each time point and $G(\tau_0)$ is the value of Eq. 1 at the initial time point.

Fabrication of hydrogel microspheres via electrospraying

Stock solutions of 20% w/v 4-arm PEG-Ac and PEG-diSH were prepared separately by dissolving them in PBS pH 5.5. PEG solutions were vortexed and briefly centrifuged to ensure complete dissolution. Next, 4-arm PEG-Ac and PEG-diSH were mixed in a 1.5 mL microcentrifuge tube and diluted with PBS pH 5.5 to achieve an equimolar ratio of acrylate:thiol end groups and a final PEG concentration of 10% w/v. This PEG precursor solution was then added to a 1 mL Luer Lock Syringe (B-D, Franklin Lakes, NJ, USA). The syringe was mounted to a syringe pump (New Era, Farmingdale, NY, USA) positioned vertically (Supplementary Fig. 4).

The PEG precursor solution was electrosprayed into a beaker filled with 100 mL of vegetable oil under constant stirring at 600 rpm to prevent PEG droplet aggregation. PEG solution was extruded at a flow rate of 20 µL/min via 30 G blunt needle tip unless otherwise specified. After ~10 min of PEG extrusion, the droplet formation phase was completed, during which no gelation occurred. Next, TEA was added to the PEG droplet/oil mixture at a final concentration of 0.2% v/v to induce gelation of PEG droplets. Gelation was allowed to proceed for 30 min to ensure complete gelation.

Following gelation, PEG microspheres were collected into 50 mL conical tubes and centrifuged for 3 min at 1000 × g. Oil was decanted from the conical tubes and 1 mL fresh PBS pH 7.4 was added to resuspend the microspheres. This suspension was again centrifuged for 3 min at 1000 × g and the supernatant decanted. The procedure was repeated five times to ensure all residual oil was removed. Washed microspheres were used for further experiments without storage.

Dip-coating of hydrogel microspheres with poly(DMA-co-SBMA)

PEG microspheres were coated with super-lubricious copolymer poly(-DMA-co-SBMA) via a dip-coating procedure. Fully washed microspheres were centrifuged for 3 min at 1000 × g and supernatant was then decanted. Poly(DMA-co-SBMA) was dissolved in pH 8.5 Tris-HCl buffer at 10 mg/mL, unless otherwise specified. Copolymer solution was then added to the microsphere pellet and gently mixed via pipetting to re-suspend the microspheres. Microcentrifuge tubes containing microspheres and copolymer solution were covered with aluminum foil and allowed to incubate for 10 min on a rotisserie shaker (MidSci, Saint Louis, MO, USA) to ensure complete mixing. Following 10 min incubation time, the microspheres were again centrifuged for 3 min at 1000 × g and the supernatant, which contained unbound copolymer, was decanted. Fresh PBS pH 7.4 was added to re-suspend microspheres for use in experiments.

Microscopy imaging of hydrogel microspheres

PEG microspheres were imaged using an inverted brightfield microscope (Axiovert 200, Zeiss, Thornwood, NY, USA) using a 10X objective. Microsphere diameter was measured using ImageJ software, where at least 50 microspheres from each sample were quantified. Fluorescent images of microspheres with varying concentrations of RhoB-labeled copolymer were also acquired and fluorescent intensity was quantified with ImageJ software. Confocal imaging (Leica Confocal SP8, Leica Microsystems, Weltzar, Germany) was performed to evaluate whether copolymer was adsorbed to just the surface of microspheres or distributed throughout the microspheres. Microspheres were coated with 1 mg/mL of poly(DMA-co-SBMA-co-RhoB) and imaged at 10X magnification.

Determination of copolymer coating stability

To determine if poly(DMA-co-SBMA-co-RhoB) remained adsorbed to the PEG hydrogel microspheres, fluorescent microscopy was performed. Microspheres were fabricated as described above, imaged at 10X magnification with a widefield fluorescence microscope following 0, 7, 14, or 21 days of incubation in 1X PBS at 37 °C. Fluorescence was again quantified using ImageJ software.

Zeta potential measurements were used to further corroborate successful adsorption of poly(DMA-co-SBMA) onto PEG hydrogel microspheres. These microspheres were fabricated as described above and incubated with either PBS or 10 mg/mL poly(DMA-co-SBMA) for 10 min at room temperature with gentle rocking. Microspheres were then centrifuged and supernatant discarded to remove non-adsorbed copolymer. Fresh 1X PBS was added to both microsphere tubes to resuspend microspheres. Zeta potential was measured thrice using a Malvern Zetasizer Advance Pro (Westborough, MA) and compared to a 10 mg/mL stock of poly(DMA-co-SBMA) without PEG microspheres.

Mechanical characterization of hydrogel microspheres

Rheological measurements of PEG microsphere with and without copolymer coating were performed using an ARES 2000ex rotational rheometer (TA Instruments, New Castle, DE, USA) with a 20 mm stainless steel parallel plate geometry. Microsphere slurry solution was pipetted directly onto a Peltier plate stage and the geometry lowered to 50 µm to ensure compression of microspheres. Storage modulus, G', and loss modulus, G'', were measured using a strain of 2% and an angular frequency of 1–10 rad/s. Shear-thinning behavior of microspheres was measured by ramping shear rate from 0.01–10 s^{-1} and fitting the measured viscosity to the Ostwald-de Waele relationship:

$$\eta = K\dot{\gamma}^{n-1} \quad (2)$$

where η is the measured viscosity, K is the flow consistency index, $\dot{\gamma}$ is the shear rate, and n is the flow behavior index. Injection force testing was performed by lowering the 20 mm parallel plate geometry at a constant rate to depress a 1 mL syringe with 27 G needle containing microsphere slurry solution, while axial force was recorded. As such, the measured axial force represented the force required to extrude the microspheres during a simulated injection.

A custom tribo-rheology setup was used to quantify the lubrication properties of the hydrogel microspheres with and without copolymer coating. Briefly, a 4.5 mm steel ball was attached to a 20 mm parallel plate geometry via gel adhesive tape. This upper ball was lowered onto three lower steel balls arranged in a triangle and held in place with a 3D-printed ball holder. The axial force applied from the upper ball onto the lower ball, as well as the rotation speed, could be controlled by the rheometer. Coefficient

of friction (COF) was measured as:

$$COF = \frac{\sqrt{2}M}{r(F+W)} \quad (3)$$

where M is the torque as measured by the rheometer, r is the radius of the steel balls (4.5 mm), F is the measured axial force, and W is the weight of the steel balls (0.33 g). For measurement of static COF, an axial force of 5 N was achieved and torque ramped until the upper ball rotated. Dynamic COF was measured by achieving an axial force of 5 N and rotating the upper ball at a constant rate of 10 s^{-1}.

Microsphere mechanical properties were compared to a simulated healthy and simulated osteoarthritic synovial fluid (SF) following the procedure by Bortel et al.[45]. Briefly, hyaluronic acid and bovine serum albumin (BSA) were mixed in DMEM/F12 at 3 mg/mL and 30 mg/mL, respectively, to simulate physiologic concentration. To represent the lower hyaluronic acid concentration and reduced viscosity associated with pathologies including osteoarthritis, simulated osteoarthritic SF was prepared using 0.3 mg/mL HA and 10 mg/mL BSA.

In vitro toxicity of microspheres

The toxicity of PEG microspheres with and without coating as well as the coating alone was evaluated by treating chondrogenic ATDC5 cells. Cells were maintained in DMEM/F12 supplemented with 10% v/v fetal bovine serum and 1% pen-strep in a humified incubator at 37 °C and 5% CO_2. Media was refreshed every 2–3 d and cells were passaged at 80% confluency. Cell proliferation was evaluated via MTS assay in four different conditions: (1) media only; (2) 100 mg/mL poly(DMA-co-SBMA-co-RhoB) in media; (3) 10% v/v PEG microspheres in media; (4) 10% v/v PEG microspheres coated with 100 mg/mL poly(DMA-co-SBMA-co-RhoB) in media. ATDC5 cells were seeded at a density of 100,000 cells/transwell insert and incubated at 37 °C for 2 h. Then, designated conditions were placed at the bottom of each well (beneath the transwell insert). Cell viability was evaluated at 24 and 72 h. To quantify cell viability, culture media in the wells was replaced with fresh media containing 10% v/v MTS reagent and incubated at 37 °C for 1 h. Following this incubation period, 100 µL of media from each well was transferred to a 96-well plate and absorbance at 490 nm was measured using a SpectraMax i3 spectrophotometer (Molecular Devices, Sunnyvale, CA). Absorbance was normalized to the media only condition, which was assumed to be 100% viability.

In vivo evaluation of microspheres

To investigate the in vivo stability and biocompatibility of the poly(-DMA-co-SBMA)-coated hydrogel microspheres, microspheres were fabricated and coated as described above, with the only difference being the incorporation of near infrared fluorescent spheres (100 nm) within the microspheres at a concentration of 0.5% w/v. Ten-week-old male C57BL6 mice were used for all in vivo experiments. Approval for using animals was obtained from Washington University School of Medicine Institutional Animal Care and Use Committee, protocol # 21-0413. Excess hairs from the abdomen and hind limbs were removed using hair removal cream. Two groups of five mice were tested, with one group receiving an injection of 20 µL of PBS + near infrared fluorescent spheres (0.5% w/v final concentration of fluorescent spheres) and the other group receiving 20 µL hydrogel microspheres slurry (500 microspheres/µL) containing 0.5% w/v near infrared fluorescent spheres. In vivo, fluorescent imaging was performed over 26 days on an IVIS spectrum CT (Revvity, Waltham, MA) using excitation/emission filters at 701 nm and 760 nm, respectively. Mice were anesthetized using isoflurane anesthesia (2% vaporized in O_2). Total radiant efficiency was measured from fixed regions of interest (ROI) over the knee joints. Analysis was completed with Living Image software (v 4.7.4, Spectral Instruments Imaging, Tuscon, AZ).

To evaluate any potential adverse effects of microsphere injection, a static weight-bearing test was conducted on the same mice described above. For this test, the mice were placed in a holder, where they were comfortably maintained while their hind paws rested on two separate sensor plates. The animals stand and naturally adjust the degree of pain by adapting the weight distribution on both rear paws.

Statistics

The results of experiments are the mean values (±standard deviation) of at least 3 individual experiments of 4–8 samples each. Comparisons between multiple groups were performed using single factor analysis of variance (ANOVA) followed by Turkey's post hoc test. Comparisons between two groups were performed with two-tailed Student's t tests and were considered statistically significant when $p < 0.05$. Statistical tests were performed with GraphPad Prism software (v9.0, San Diego, CA).

Data Availability

Data sets generated during the current study are available from the corresponding author on reasonable request.

Received: 14 October 2024; Accepted: 25 January 2025;
Published online: 24 March 2025

References

1. Geng, R. et al. Knee osteoarthritis: current status and research progress in treatment (Review). *Exp. Ther. Med.* **26**, 481 (2023).
2. Sharma, L. Osteoarthritis of the Knee. *N. Engl. J. Med.* **384**, 51–59 (2021).
3. Yelin, E., Weinstein, S. & King, T. The Burden of Musculoskeletal Diseases in the United States, *Semin. Arthrit. Rheum.* **46**, 259–260 (2018).
4. Hawker, G. A. International, osteoarthritis: a serious disease. *Clin. Exp Rheumatol.* **120**, 3–6 (2019).
5. Lim, W. B. & Al-Dadah, O. Conservative treatment of knee osteoarthritis: a review of the literature. *World J. Orthop.* **13**, 212–229 (2022).
6. Migliore, A. & Procopio, S. Effectiveness and utility of hyaluronic acid in osteoarthritis. *Clin. Cases Miner. Bone Metab* **12**, 31–33 (2015).
7. Shahid, A. et al. Do platelet-rich plasma injections for knee osteoarthritis work? *Cureus* **15**, e34533 (2023).
8. Jain, E. et al. Platelet-rich plasma released from polyethylene glycol hydrogels exerts beneficial effects on human chondrocytes. *J. Orthop. Res.* **37**, 2401–2410 (2019).
9. Siefen, T., Bjerregaard, S., Borglin, C. & Lamprecht, A. Assessment of joint pharmacokinetics and consequences for the intraarticular delivery of biologics. *J. Controlled Release* **348**, 745–759 (2022).
10. Coaccioli, S., Sarzi-Puttini, P., Zis, P., Rinonapoli, G. & Varrassi, G. Osteoarthritis: new Insight on Its pathophysiology. *J. Clin. Med.* **11**, 6013 (2022).
11. Yao, Y., Wei, G., Deng, L. & Cui, W. Visualizable and Lubricating Hydrogel Microspheres Via NanoPOSS for Cartilage Regeneration. *Adv. Sci.* **10**, 2207438 (2023).
12. Wang, S., Qiu, Y., Qu, L., Wang, Q. & Zhou, Q. Hydrogels for treatment of different degrees of osteoarthritis. *Front Bioeng. Biotechnol.* **10**, 858656 (2022).
13. Lei, Y. et al. Stem cell-recruiting injectable microgels for repairing osteoarthritis. *Adv. Function. Mater.* **31**, 2105084 (2021).
14. Han, Y. et al. Biomimetic injectable hydrogel microspheres with enhanced lubrication and controllable drug release for the treatment of osteoarthritis. *Bioact. Mater.* **6**, 3596–3607 (2021).
15. Hamilton, M., Wang, J., Dhar, P. & Stehno-Bittel, L. Controlled-release hydrogel microspheres to deliver multipotent stem cells for treatment of knee osteoarthritis. *Bioengineering* **10**, 1315 (2023).

16. Kroger, S. M. et al. Design of hydrolytically degradable polyethylene glycol crosslinkers for facile control of hydrogel degradation. *Macromol. Biosci.* **20**, 2000085 (2020).
17. Zustiak, S. P. & Leach, J. B. Hydrolytically Degradable Poly(Ethylene Glycol) hydrogel scaffolds with tunable degradation and mechanical properties. *Biomacromolecules* **11**, 1348–1357 (2010).
18. Herrick, W. G. et al. PEG-Phosphorylcholine hydrogels as tunable and versatile platforms for mechanobiology. *Biomacromolecules* **14**, 2294–2304 (2013).
19. Ghassemi, Z., Ruesing, S., Leach, J. B. & Zustiak, S. P. Stability of proteins encapsulated in Michael-type addition polyethylene glycol hydrogels. *Biotechnol. Bioeng.* **118**, 4840–4853 (2021).
20. Jain, E., Hill, L., Canning, E., Sell, S. A. & Zustiak, S. P. Control of gelation, degradation and physical properties of polyethylene glycol hydrogels through the chemical and physical identity of the crosslinker. *J. Mater. Chem. B* **5**, 2679–2691 (2017).
21. Rossow, T. et al. Controlled synthesis of cell-laden microgels by radical-free gelation in droplet microfluidics. *J. Am. Chem. Soc.* **134**, 4983–4989 (2012).
22. Sheth, S., Stealey, S., Morgan, N. Y. & Zustiak, S. P. Microfluidic chip device for in situ mixing and fabrication of hydrogel microspheres via Michael-type addition. *Langmuir* **37**, 11793–11803 (2021).
23. Li, F., Wang, A. & Wang, C. Analysis of friction between articular cartilage and polyvinyl alcohol hydrogel artificial cartilage. *J. Mater. Sci. Mater. Med.* **27**, 87 (2016).
24. Echeverría, C. & Mijangos, C. Rheology applied to microgels: brief (Revision of the) state of the art. *Polymers* **14**, 1279 (2022).
25. Seong, Y. J. et al. Hyaluronic acid-based hybrid hydrogel microspheres with enhanced structural stability and high injectability. *ACS Omega* **4**, 13834–13844 (2019).
26. Li, Z. et al. High drug loading hydrophobic cross-linked dextran microspheres as novel drug delivery systems for the treatment of osteoarthritis. *Asian J. Pharm. Sci.* **18**, 100830 (2023).
27. Lei, Y. et al. Injectable hydrogel microspheres with self-renewable hydration layers alleviate osteoarthritis. *Sci. Adv.* **8**, eabl6449 (2022).
28. Lin, W. & Klein, J. Recent progress in cartilage lubrication. *Adv. Mater.* **33**, 2005513 (2021).
29. Wong, M. & Carter, D. R. Articular cartilage functional histomorphology and mechanobiology: a research perspective. *Bone* **33**, 1–13 (2003).
30. Xiao, P. et al. Reprogramming macrophages via immune cell mobilized hydrogel microspheres for osteoarthritis treatments. *Bioactive Mater.* **32**, 242–259 (2024).
31. Miao, K. et al. Microenvironment-responsive bilayer hydrogel microspheres with gelatin-shell for osteoarthritis treatment. *Int. J. Biol. Macromol.* **261**, 129862 (2024).
32. Loutfy, R. O. Fluorescence probes for polymerization reactions: Bulk polymerization of styrene, n-butyl methacrylate, ethyl methacrylate, and ethyl acrylate. *J. Polymer Sci. Polymer Phys. Edn.* **20**, 825–835 (1982).
33. Bou, S., Klymchenko, A. S. & Collot, M. Fluorescent labeling of biocompatible block copolymers: synthetic strategies and applications in bioimaging. *Mater. Adv* **2**, 3213–3233 (2021).
34. Yang, J. et al. Ball-bearing-inspired polyampholyte-modified microspheres as bio-lubricants attenuate osteoarthritis. *Small* **16**, 2004519 (2020).
35. Galluccio, F. et al. The booster effect of a single quarterly dose of hyaluronic acid in knee osteoarthritis: five-year results of a registry-based study. *Cureus* **14**, e31592 (2022).
36. Doan, T. N., Bernard, F. C., McKinney, J. M., Dixon, J. B. & Willett, N. J. Endothelin-1 inhibits size dependent lymphatic clearance of PEG-based conjugates after intra-articular injection into the rat knee. *Acta Biomater* **93**, 270–281 (2019).
37. Tong, X., Lee, S., Bararpour, L. & Yang, F. Long-term controlled protein release from Poly(Ethylene Glycol) hydrogels by modulating mesh size and degradation. *Macromol. Biosci.* **15**, 1679–1686 (2015).
38. Choi, M. H. et al. Micro-clotting of platelet-rich plasma upon loading in hydrogel microspheres leads to prolonged protein release and slower microsphere degradation. *Polymers* **12**, 1712 (2020).
39. Daniel, D. et al. Hydration lubrication of polyzwitterionic brushes leads to nearly friction- and adhesion-free droplet motion. *Commun. Phys.* **2**, 105 (2019).
40. Wang, H., Zhang, Y., Sun, Y., Liu, D. & Cao, Y. Excellent hydration lubrication based on Zwitterionic Poly (N-vinylpyrrolidone-co-methacrylic acid) for hair combing improvement. *Surf. Interfaces* **48**, 104242 (2024).
41. Ahmed, A. M., Burke, D. L. & Yu, A. In-vitro measurement of static pressure distribution in synovial joints-Part II: Retropatellar surface. *J. Biomech. Eng.* **105**, 226–236 (1983).
42. Cao, F., Tan, L., Xiang, L., Liu, S. & Wang, Y. Application of the copolymers containing sulfobetaine methacrylate in protein separation by capillary electrophoresis. *J. Biomater. Sci. Polymer Edin.* **24**, 2058–2070 (2013).
43. Ward, J. W., Cramm, J., Peter E. R. & Johnson, S. B. Derivatized Rhodamine Dye and its Copolymers, Patent #WO1998002492A1 (1998).
44. Magde, D., Elson, E. & Webb, W. W. Thermodynamic fluctuations in a reacting system-measurement by fluorescence correlation spectroscopy. *Phys. Rev. Lett.* **29**, 705–708 (1972).
45. Bortel, E. L., Charbonnier, B. & Heuberger, R. Development of a synthetic synovial fluid for tribological testing. *Lubricants* **3**, 664–686 (2015).

Acknowledgements

The authors would like to thank Julie Prior from the Washington University in Saint Louis Molecular Imaging Center for assistance with IVIS imaging. Funding for this project was provided by NIH grant 5RO1AR081270-02, as well as Foundational Interdisciplinary Research Experience for Undergraduates at Saint Louis University and the Kern Entrepreneurial Engineering Network (KEEN).

Author contributions

S.P.Z., S.S., P.J., and Y.A.A. conceived and designed all experiments. S.S., E.D., A.S., M.H., and M.B., A.M.T. performed all data collection and analysis. S.S., A.M.T., E.D., and S.P.Z. wrote the main manuscript text. All authors contributed to manuscript revisions and final data analysis.

Competing interests

S.P.Z. is an associate editor for *npj Biomedical Innovations* and also guest editor for the 'Bioengineering innovations in osteoarthritis treatment' collection.

Additional information

Supplementary information The online version contains supplementary material available at https://doi.org/10.1038/s44385-025-00011-3.

Correspondence and requests for materials should be addressed to Silviya Petrova Zustiak.